



Hydriding behavior of gas-atomized AB₅ alloys

R.C. Bowman Jr.^{a,*}, C. Witham^a, B. Fultz^a, B.V. Ratnakumar^b, T.W. Ellis^c, I.E. Anderson^c

^aDivision of Engineering and Applied Science, California Institute of Technology Pasadena, CA 91125 USA

^bElectrochemical Technologies Group, 4800 Oak Grove Dr., Jet Propulsion Laboratory Pasadena, CA 91109 USA

^cAmes Laboratory, Iowa State University Ames, IA 50011 USA

Abstract

The hydriding characteristics of some AB₅ alloys produced by high pressure gas atomization (HPGA) have been examined during reactions with hydrogen gas, and in electrochemical cells. The hydrogen storage capacities and the equilibrium pressures for HPGA processed LaNi₅, LaNi_{4.75}Sn_{0.25}, and MmNi_{3.5}Co_{0.8}Al_{0.4}Mn_{0.3} alloys (where Mm denotes Mischmetal) are found to be nearly identical to annealed alloys produced as ingots. The large discontinuous volume change across the α - β plateau region for gas-atomized LaNi₅H_x was seen to produce extensive fracturing in all but the smallest alloy spheres. However, only the largest spheres of the gas-atomized MmNi_{3.5}Co_{0.8}Al_{0.4}Mn_{0.3} and LaNi_{4.75}Sn_{0.25}H_x alloys exhibited any discernible fracturing. The maximum electrochemical storage capacities of the gas-atomized LaNi_{4.75}Sn_{0.25} and MmNi_{3.5}Co_{0.8}Al_{0.4}Mn_{0.3} alloys were found to be smaller than the capacities of annealed alloys prepared from ingots.

Keywords: Metal hydrides; Gas atomization; Electrochemical hydride properties; hydrogen storage alloys; Ni-MH battery alloys; LaNi₅

1. Introduction

Rare earth AB₅ Haucke phase alloys are being used extensively in negative electrodes of rechargeable nickel-metal hydride (Ni-MH) batteries. Sakai et al. [1–3] have described the importance of alloy composition, stoichiometry, and microstructure on both electrode performance and durability during electrochemical charge-discharge cycling. In particular, variations in alloy casting conditions and thermal processing have been shown [1–3] to influence hydrogen absorption-desorption properties and cycle life of Mischmetal (Mm) based AB₅ alloys. The recently developed high-pressure gas atomization (HPGA) processing technology [4] may offer benefits associated with rapid-solidification effects, which could enhance Ni-MH battery performance characteristics with lower cost Mm-based alloys. HPGA is being explored as a substitute for the common commercial practice of manufacturing LaNi₅ powders from chill-cast ingots that must be extensively annealed to homogenize the cast microstructure prior to mechanical crushing and grinding. An expected advantage for HPGA alloys would be homogeneity of the rapidly solidified microstructure [4] that should yield improved hydrogen capacities and less variability in the plateau pressures.

The present study was planned to evaluate the hydriding behavior of some representative AB₅ alloys produced by the HPGA method during gas-phase reactions and during electrochemical cycling in alkaline solutions. These results are compared to measurements performed on similar alloys that were prepared by conventional methods. The specific systems investigated include LaNi₅, MmNi_{3.5}-Co_{0.8}Al_{0.4}Mn_{0.3} (which corresponds to a particularly robust alloy for electrochemical cycling [2]), and LaNi_{4.75}Sn_{0.25}. Substituting tin (Sn) for Ni in LaNi₅ has been found to enhance greatly the capacity retention of the material during both thermal cycling with hydrogen gas [5] and in electrochemical cells [6]. The best hydrogen storage capacity and cyclic lifetimes for annealed, arc-melted LaNi_{5-y}Sn_y alloys during electrochemical reactions were found for y=0.25 [6]. This Sn composition should therefore serve as a good test of the properties of materials prepared by HPGA.

2. Experimental details

High yields of fine (less than 20 μ m diameter) spherical powders of rare-earth AB₅ alloys were produced with the previously described [4] Ames Laboratory HPGA system. Argon gas traveling at a speed of about Mach three was used to disintegrate the stream of molten alloys into the

*Corresponding author.

droplets. Scanning electron micrographs of the particle shapes and size distributions for as-prepared gas-atomized (GA) LaNi_5 and $\text{MmNi}_{3.5}\text{Co}_{0.8}\text{Al}_{0.4}\text{Mn}_{0.3}$ alloys are shown in Fig. 1(a and c respectively). X-ray diffraction (XRD) patterns were obtained using an INEL CPS-120 powder diffractometer with $\text{Co K}\alpha$ radiation. XRD revealed GA- LaNi_5 to be single phase with high crystalline quality as indicated by very sharp diffraction peaks while the GA- $\text{MmNi}_{3.5}\text{Co}_{0.8}\text{Al}_{0.4}\text{Mn}_{0.3}$ and $\text{LaNi}_{4.75}\text{Sn}_{0.25}$ alloys gave XRD patterns with broadened peaks and indications of small quantities of secondary phases. Additional characterizations of the microstructure for GA- LaNi_5 are reported by Anderson et al. [4].

The pressure-composition-temperature (p-c-T) data were obtained with an automated version of a previously described [5] all-metal Sieverts' gas-volumetric apparatus. Surface areas of as-produced and activated, gas-cycled powders were determined by the Brunauer-Emmett-Teller (BET) technique using nitrogen gas in a Micromeritics Model 2360 analyzer.

The electrodes for the cyclic electrochemical lifetime studies contained 76% activated alloy powder, 19% INCO nickel powder as a conductive diluent, and 5% Teflon binder pressed at 570 K onto an expanded nickel screen. $\text{NiOOH}/\text{Ni}(\text{OH})_2$ served as the counter electrode and a Hg/HgO reference electrode was also used. The electrodes were contained in an o-ring sealed, flooded prismatic glass cell with a 31 wt% KOH electrolyte solution. The cell assembly and measurement procedures have been thoroughly described elsewhere [6].

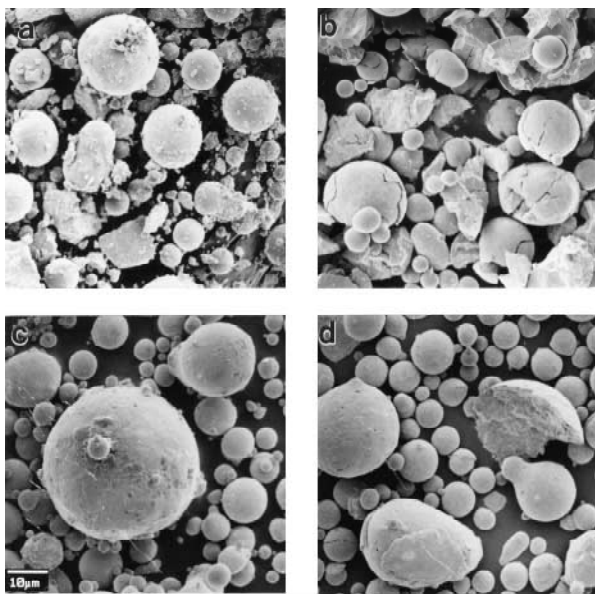


Fig. 1. Scanning electron microscopy micrographs of gas-atomized alloys: (a) as-prepared LaNi_5 ; (b) GA- LaNi_5 after activation and five hydrogen absorption-desorption cycles; (c) as-prepared $\text{MmNi}_{3.5}\text{Co}_{0.8}\text{Al}_{0.4}\text{Mn}_{0.3}$ alloy; and (d) GA- $\text{MmNi}_{3.5}\text{Co}_{0.8}\text{Al}_{0.4}\text{Mn}_{0.3}$ after ten hydrogen absorption-desorption cycles following activation.

3. Results and discussion

The room temperature hydrogen absorption and desorption isotherms for GA- LaNi_5 activated by an initial absorption-desorption cycle are shown in Fig. 2. The excellent reproducibility between the first and fifth cycles confirms that equilibrium conditions have been established during these runs. Fig. 2 also presents the 300 K isotherm data previously measured at the University of Vermont by Luo et al. [7] on a high purity $\text{LaNi}_{5.00}$ sample prepared by arc-melting and annealed at 1223 K for 100 h. No discernable differences in total hydrogen capacity, plateau pressures, hysteresis, or width of the α - β region are noted between the unannealed gas-atomized and annealed arc-melted materials.

Fig. 1b illustrates that extensive fracturing had occurred in the GA- LaNi_5 particles with diameters greater than 10–15 μm . Substantial broadening of the XRD peaks, which corresponds to particle size reduction and microstrains induced during hydriding [8], was observed following the isotherm measurements. Furthermore, the BET surface area of the as-prepared GA- LaNi_5 alloy increased from $0.04 \text{ m}^2 \text{ g}^{-1}$ to $0.22 \text{ m}^2 \text{ g}^{-1}$ after the fifth p-c-T isotherm, which was essentially identical to the $0.21 \text{ m}^2 \text{ g}^{-1}$ surface area determined on the annealed arc-melted LaNi_5 material after the isotherm measurement shown in Fig. 2. Evidently the nominal 25% unit cell volume expansion across α - β region for the GA- LaNi_5 particles produces fracturing and decrepitation when the diameters of the spherical particles exceed about 10 μm .

Due to the widespread commercial interest in Mm-based alloys for Ni-MH batteries, a gas-atomized

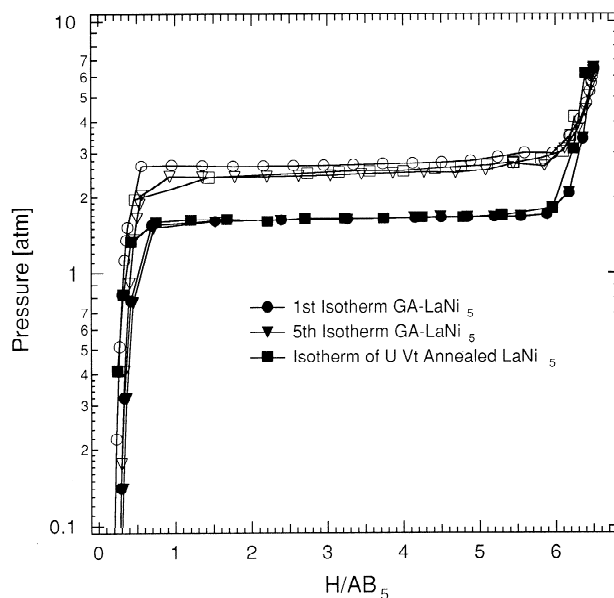


Fig. 2. Comparison of hydrogen absorption (open symbols) and desorption (closed symbols) room temperature isotherms for 1223 K annealed arc-melted and unannealed gas-atomized LaNi_5 .

$\text{MmNi}_{3.5}\text{Co}_{0.8}\text{Al}_{0.4}\text{Mn}_{0.3}$ alloy was produced by HPGA. Hydrogen absorption–desorption isotherms were determined at three temperatures after activation. These results are presented in Fig. 3. The plateau pressures for this gas-atomized alloy have significant slopes and hysteresis. Nevertheless, the isotherm for 313 K in Fig. 3 corresponds much more closely to the isotherm reported by Sakai et al. [2] for induction melted and melt-spun $\text{MmNi}_{3.5}\text{Co}_{0.8}\text{Al}_{0.4}\text{Mn}_{0.3}$ alloys than for their gas-atomized powder. Our HPGA method apparently produced a more homogenous composition than the process previously used by Sakai et al. The scanning electron micrograph in Fig. 1d shows that only the largest spheres in the activated GA- $\text{MmNi}_{3.5}\text{Co}_{0.8}\text{Al}_{0.4}\text{Mn}_{0.3}$ alloy experience any discernible fracturing, perhaps because of the much narrower α - β region for this alloy. No significant increases were noted in the XRD peak broadening following these hydriding reactions.

The storage capacities during room temperature cycling of electrochemical cells fabricated from the GA- $\text{MmNi}_{3.5}\text{Co}_{0.8}\text{Al}_{0.4}\text{Mn}_{0.3}$ alloy activated by one or ten gas-phase absorption–desorption cycles are presented in Fig. 4. The maximum electrochemical storage capacities of these cells with HPGA $\text{MmNi}_{3.5}\text{Co}_{0.8}\text{Al}_{0.4}\text{Mn}_{0.3}$ were only about 100–120 mAh g^{-1} , which is well below the maximum capacity of 250 mAh g^{-1} shown in Fig. 4 for an induction melted alloy of similar composition obtained under identical conditions. It is possible that the poor electrochemical behavior of the gas-atomized AB_5 alloy results from the lack of fracturing of stable and tenacious surface corrosion films since the activation procedures generated very little fracturing as shown in Fig. 1d.

Hydrogen absorption and desorption isotherms were

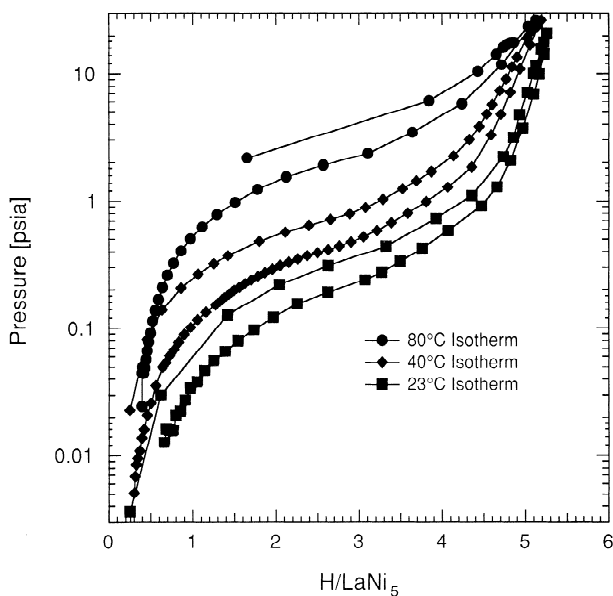


Fig. 3. Hydrogen absorption–desorption isotherms for an unannealed gas-atomized $\text{MmNi}_{3.5}\text{Co}_{0.8}\text{Al}_{0.4}\text{Mn}_{0.3}$ alloy.

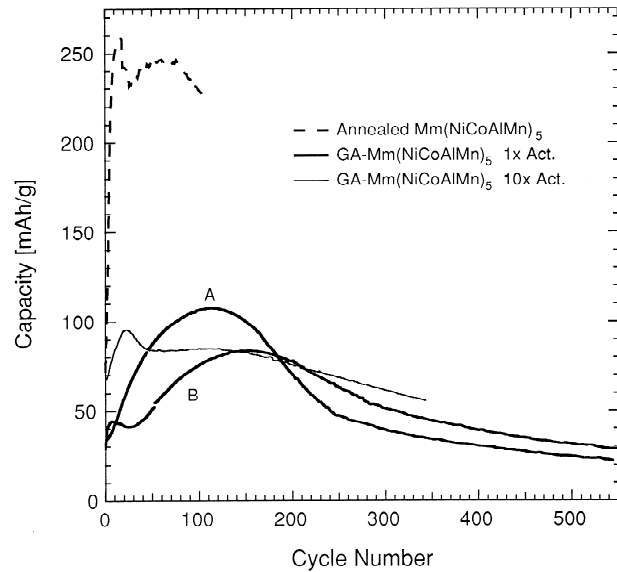


Fig. 4. Comparison of electrochemical storage capacities for activated (1 cycle and 10 cycles) gas-atomized $\text{MmNi}_{3.5}\text{Co}_{0.8}\text{Al}_{0.4}\text{Mn}_{0.3}$ and an activated commercial $\text{Mm}(\text{NiCoAlMn})_5$ alloy prepared by induction melting.

measured at room temperature (i.e., 296 K) for unannealed GA- $\text{LaNi}_{4.75}\text{Sn}_{0.25}$ after five activation cycles. These results are compared in Fig. 5 to the room temperature (i.e., 300 K) isotherms obtained by Luo et al. [9] on annealed arc-melted $\text{LaNi}_{5-y}\text{Sn}_y$ with $y=0.1, 0.25,$ and 0.32 . Although the hydrogen storage capacities for both $y=0.25$ alloys are nearly identical, the isotherms for the

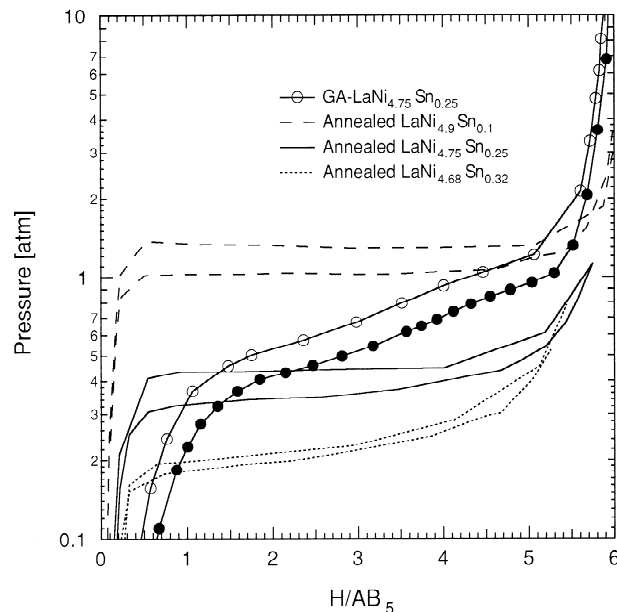


Fig. 5. Comparison of hydrogen absorption (open symbols) and desorption (closed symbols) room temperature isotherms for unannealed gas-atomized $\text{LaNi}_{4.75}\text{Sn}_{0.25}$ alloy and for annealed arc-melted $\text{LaNi}_{5-y}\text{Sn}_y$ with $y=0.1, 0.25,$ and 0.32 determined by Luo et al. [9].

HPGA material exhibit rather steep slopes across the plateau region and a larger hysteresis ratio. Luo et al. [9] found very similar differences between unannealed and annealed (1073 K for 3 d) arc-melted $\text{LaNi}_{4.77}\text{Sn}_{0.23}$, which is commonly attributed [5,9,10] to an inhomogeneous distribution of Sn within the microstructure. This interpretation is consistent with the plateau pressures given in Fig. 5 for Sn compositions between $y=0.1$ and $y=0.32$. It is also consistent with the broadened XRD peaks for the $\text{GA-LaNi}_{4.75}\text{Sn}_{0.25}$ compared to either GA-LaNi_5 or annealed $\text{LaNi}_{5-y}\text{Sn}_y$. Although the sloping plateau for $\text{GA-LaNi}_{4.75}\text{Sn}_{0.25}$ is nearly as wide as for GA-LaNi_5 , scanning electron micrographs after five activation cycles revealed no fracturing for particles up to 40 μm in diameter. In addition, the surface area only increased from an initial value of $0.06 \text{ m}^2 \text{ g}^{-1}$ for the as-prepared powder to $0.09 \text{ m}^2 \text{ g}^{-1}$ following the activation cycles. As seen in the GA-Mm alloy, activation did not change the XRD peaks of the $\text{GA-LaNi}_{4.75}\text{Sn}_{0.25}$ alloy. Hence an inhomogeneous distribution of Sn appears to prevent microcracking upon hydrogenation at least as well as a homogeneous distribution.

The electrochemical cycling behavior for two cells prepared with unannealed $\text{GA-LaNi}_{4.75}\text{Sn}_{0.25}$ are compared in Fig. 6 to the capacity for an electrode produced with annealed arc-melted $\text{LaNi}_{4.75}\text{Sn}_{0.25}$. The HPGA alloy required nearly 20 cycles to give a maximum capacity of $225\text{--}250 \text{ mA g}^{-1}$ while the annealed, arc-melted alloy achieved 315 mA g^{-1} within five electrochemical cycles. The reduced capacity for the HPGA alloy can be readily attributed to its sloping isotherms where one atmosphere pressure is reached at a hydrogen composition of $x=5.0$ while one atmosphere is not reached until $x=5.7$ for the annealed alloy (Fig. 5). An electrochemical capacity at

least 15% smaller is therefore predicted for the HPGA alloy. Furthermore, the capacity retention of the HPGA alloy during electrochemical cycling is seen to be less than for the arc-melted alloy (Fig. 6), which when combined with the slower activation also contributes to a reduced maximum capacity. Further discussion of the electrochemical degradation of the HPGA alloys will be presented elsewhere.

In conclusion, GA-AB_5 powders produced by the HPGA method have gas-phase hydrogen storage capacities and equilibrium pressures similar to materials prepared from annealed ingots [2,5,7–9]. When used in electrochemical cells, however, unannealed HPGA $\text{MmNi}_{3.5}\text{Co}_{0.8}\text{Al}_{0.4}\text{Mn}_{0.3}$ and $\text{LaNi}_{4.75}\text{Sn}_{0.25}$ have reduced capacities and more rapid degradation than conventionally processed alloys. It is anticipated that substantial improvement in these electrochemical properties can be obtained by appropriate annealings [3] of the gas-atomized alloys. These studies are in progress.

Acknowledgments

The authors thank Fran Laabs (Ames Lab) for the scanning electron microscopy measurements and Prof. Ted Flanagan (U. Vermont) for providing his isotherm data on the annealed $\text{LaNi}_{5-y}\text{Sn}_y$ alloys. These studies were performed under funding provided by the DOE Grant DE-FG03-94ER14493. The Jet Propulsion Laboratory is operated by Caltech under contract with the U.S. National Aeronautics and Space Administration. Ames Laboratory is operated by Iowa State University for the U.S. Department of Energy under Contract No. W-7405-Eng-82.

References

- [1] T. Sakai, H. Yoshinaga, H. Miyamura, N. Kuriyama and H. Ishikawa, *J. Alloys Compounds*, **180** (1992) 37.
- [2] T. Sakai, H. Miyamura, N. Kuriyama, H. Ishikawa and I. Uehara, *Z. Phys. Chem.*, **183** (1994) 333.
- [3] T. Sakai, M. Matsuoka and C. Iwakura, in K.A. Gschneider and L. Eyring (eds.), *Handbook on the Physics and Chemistry of Rare Earths*, Vol. 21, Elsevier, Amsterdam, 1995, p. 133.
- [4] I.E. Anderson, M.G. Osborne and T.W. Ellis, *JOM* **48**, No. 3 (1996) 38.
- [5] R.C. Bowman Jr., C.H. Luo, C.C. Ahn, C.K. Witham and B. Fultz, *J. Alloys Compounds*, **217** (1995) 185.
- [6] B.V. Ratnakumar, C. Witham, R.C. Bowman Jr., A. Hightower and B. Fultz, *J. Electrochem. Soc.*, **143** (1996) 2578.
- [7] W. Luo, S. Luo, J. Clewley, T. Flanagan, R. Bowman and J. Cantrell, *J. Alloys Compounds*, **202** (1993) 147.
- [8] A. Percheron-Guegan, C. Lartique, J.C. Achard, P. Germi and F. Tasset, *J. Less-Common Met.*, **74** (1980) 1.
- [9] S. Luo, W. Luo, J.D. Clewley, T.B. Flanagan and L.A. Wade, *J. Alloys Compounds*, **231** (1995) 467.
- [10] S. Luo, W. Luo, J.D. Clewley, T.B. Flanagan and R.C. Bowman Jr., *J. Alloys Compounds*, **231** (1995) 473.

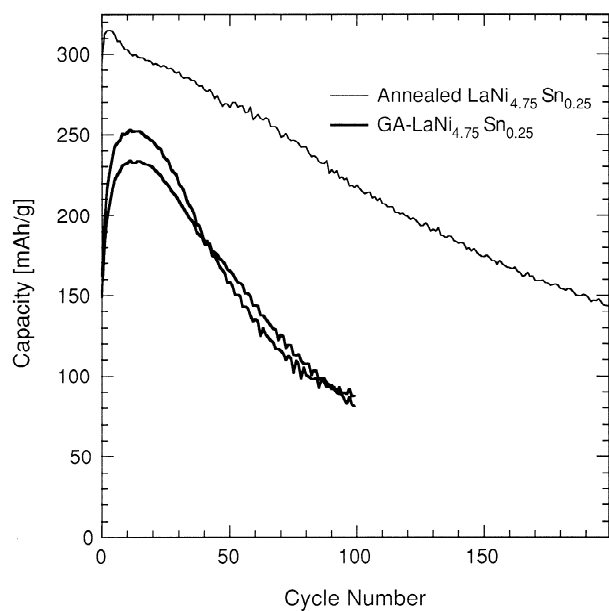


Fig. 6. Comparison of electrochemical storage capacities for the activated gas-atomized and annealed arc-melted $\text{LaNi}_{4.75}\text{Sn}_{0.25}$ alloys.